DOI 10.5012/bkcs.2011.32.2.467

Analysis of Spin Exchange Interactions in $(C_2N_2H_{10})[Fe(HPO_3)F_3]$ on the Basis of Electronic Structure Calculations

Hyun-Joo Koo

Department of Chemistry and Research Institute for Basic Sciences, Kyung Hee University, Seoul 130-701, Republic of Korea
E-mail: hjkoo@khu.ac.kr
Received October 28, 2010, Accepted November 29, 2010

Spin exchange interactions of $(C_2N_2H_{10})[Fe(HPO_3)F_3]$ were examined by performing a spin dimer analysis based on extended Hückel tight binding method and a mapping analysis based on first principles density functional theory. Spin exchange interactions occur through the super-superexchange paths J_1 and J_2 in $(C_2N_2H_{10})[Fe(HPO_3)F_3]$. In the super-superexchange path J_2 magnetic orbital interactions between e_g-block levels are much stronger than those from t_{2g}-block levels. Both electronic structure calculations show that the spin exchange interaction through the super-superexchange path J_2 is much stronger than that of J_1.

Key Words: Spin dimer analysis, Mapping analysis, Magnetic orbital, $(C_2N_2H_{10})[Fe(HPO_3)F_3]$, Super-Super exchange

Introduction

New transition metal phosphite template ethylenediammonium $(C_2N_2H_{10})[Fe(HPO_3)F_3]$ has been synthesized and characterized by single crystal X-ray diffraction.[1-2] The crystal structure of $(C_2N_2H_{10})[Fe(HPO_3)F_3]$ consists of octahedral FeO_3F_3 and pseudopyramidal $(HPO_3)^{2-}$ phosphite oxoanions (Figure 1a). The trans-oxygen atoms in the basal plane of FeO_3F_3 octahedron are shared by $(HPO_3)^{2-}$ units, so it forms $[Fe(HPO_3)F_3)]^{2-}$ anionic chains along the c-direction.[2] Two anionic chains of $[Fe(HPO_3)F_3)]^{2-}$ are condensed by corner-sharing between $(HPO_3)^{2-}$ and $[FeO_3F_3]$ provided from each $[Fe(HPO_3)F_3)]^{2-}$ chain (Figure 1b). Namely, three oxygen atoms of each isolated $[FeO_3F_3]$ octahedron are connected by corner-sharing with neighboring three $(HPO_3)^{2-}$ units and vice versa three oxygen atoms of $(HPO_3)^{2-}$ unit are connected by corner-sharing with neighboring three $[FeO_3F_3]$ octahedra. Thus, it forms a zigzag chain made up of isolated $[FeO_3F_3]$ units along the c-direction (Figure 1b). These zigzag chains are well separated by ethylenediammonium dications $(C_2N_2H_{10})^{2+}$ (Figure 1a). In the $[Fe(HPO_3)F_3)]^{2-}$ anionic chain, Fe^{3+} (d^5) ion has unpaired spins of 5/2. Since the isolated $[FeO_3F_3]$ units are connected by $(HPO_3)^{2-}$ units, there are two super-superexchange paths J_1 and J_2 in the $[Fe(HPO_3)F_3)]^{2-}$ anionic chain (Figure 1b). In the super-superexchange path J_1, two adjacent Fe^{3+} ions are linked by two $(HPO_3)^{2-}$ units, while in the super-superexchange path J_2, two adjacent Fe^{3+} ions are linked by one $(HPO_3)^{2-}$ unit. Magnetic properties of $(C_2N_2H_{10})[Fe(HPO_3)F_3]$ were explored by conducting electron spin resonance spectroscopy and magnetic susceptibility measurement.[2] Both experimental measurements indicate antiferromagnetic coupling in $(C_2N_2H_{10})[Fe(HPO_3)F_3]$. From the Curie-Weiss plot, Fernández-Armas *et al.*[2] obtained Curie-Weiss temperature of −28.0 K and Curie constant of 4.38 cm^3 K mol^{-1}. In addition, the magnetic susceptibility data have been fitted by using a linear chain model with second nearest neighbor interaction and the best fitting result obtained with J_1 = −1.63 K and J_2 = −0.87 K,[2] respectively.

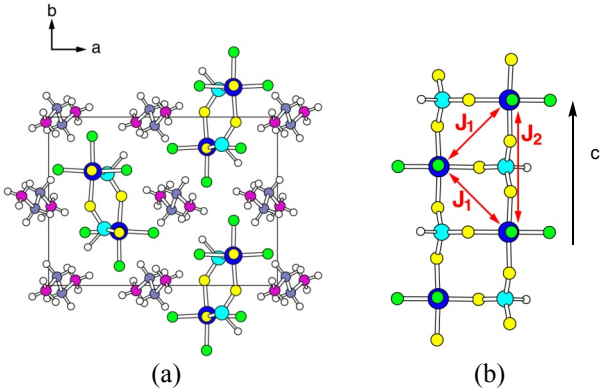

Figure 1. (a) Projective view of the crystal structure of $(C_2N_2H_{10})[Fe(HPO_3)F_3]$, where the blue, cyan, green, yellow, gray, purple and white circles indicate Fe, P, F, O, C, N and H atoms, respectively. (b) $[Fe(HPO_3)F_3]$ double chain along the c-direction, where the J_1 and J_2 represent the SSE paths.

In general, spin exchange interactions between adjacent spin sites take place through M-L-M superexchange (SE) paths or M-L···L-M super-superexchange (SSE) paths, where M is transition metal site and L is surrounded ligands. Strongly interacting spin exchange paths of a magnetic solid are determined by the overlap between magnetic orbitals in a spin dimer (i.e. structural units containing two spin sites).[3-7] The strength of SSE interaction of a spin dimer increases with increasing the overlap between the magnetic orbital (i.e. singly occupied molecular orbital containing unpaired spin) of a given spin dimer. So, the strongly interacting spin unit of a magnetic solid does not necessarily have the same geometrical feature as does the arrangement of its magnetic ions or spin-carrying molecules.[4,6-7] To investigate magnetic properties of a given magnetic solid, we need to determine a spin lattice model made up of strongly interacting spin dimer units and responsible for its magnetic behavior. The magnetic susceptibility data of $(C_2N_2H_{10})[Fe$

$(HPO_3)F_3$] have been reproduced with two spin exchange parameters J_1 and J_2. Magnetic susceptibility data measured experimentally can be reproduced equally well with more than one spin exchange parameter sets since the spin exchange parameters act as numerical fitting parameters.[8] In the fitting analysis, the spin exchange parameters are assigned without consideration for a characteristic of electronic structure of spin exchange paths. Therefore, to determine a precise spin lattice model responsible for magnetic properties of a magnetic solid it is necessary to evaluate spin exchange parameters on the basis of appropriate electronic structure calculations.[9] The magnetic properties of $(C_2N_2H_{10})$[$Fe(HPO_3)F_3$], however, have not been studied on the basis of electronic structure calculations. In the present work, we evaluate spin exchange parameters of $(C_2N_2H_{10})$[$Fe(HPO_3)F_3$] by performing spin dimer analysis based on extended Hückel tight binding (EHTB) calculations as well as mapping analysis based on first principles density functional electronic band structure calculations.

Spin Dimer Anaysis

In spin dimer analysis based on EHTB calculations, the strength of an antiferromagnetic (AFM) interaction between two spin sites is estimated by considering the AFM spin exchange parameter J_{AF},[3,10]

$$J_{AF} \approx - \frac{<(\Delta e)^2>}{U_{eff}} \quad (1)$$

where U_{eff} is the effective on-site repulsion that is essentially a constant for a given compound. The $<(\Delta e)^2>$ term is calculated by performing EHTB electronic structure calculations[11-12] for a spin dimer, which is given by adjacent octahedra $(FeO_3F_3)\cdots(FeO_3F_3)$ for the magnetic solid $(C_2N_2H_{10})$[$Fe(HPO_3)F_3$]. The d-block levels of an (FeO_3F_3) octahedron are split into the e_g and t_{2g} levels and the electronic configuration of Fe^{3+} ion is the $(t_{2g})^3(e_g)^2$. When we use the orbitals ϕ_1, ϕ_2, and ϕ_3 to describe the three orbitals of the t_{2g} level, ϕ_4 and ϕ_5 to describe the two orbitals of the e_g level, the $<(\Delta e)^2>$ term is approximated by[3]

$$<(\Delta e)^2> \approx \frac{1}{N^2}\left[\left(\frac{n_t}{3}\right)^2 \sum_{\mu=1}^{3}\left(\Delta e_{\mu\mu}\right)^2 + \left(\frac{n_e}{2}\right)^2 \sum_{\mu=4}^{5}\left(\Delta e_{\mu\mu}\right)^2\right] \quad (2)$$

where n_e and n_t are the numbers of electrons in the e_g and t_{2g} levels, respectively, N is the total number of d-electrons each Fe^{3+} cation has (i.e., $N = n_e + n_t$), and $\Delta e_{\mu\mu}$ is the energy split that results when two magnetic orbitals ϕ_μ ($\mu = 1-5$) on adjacent spin sites interact. In the present work, the $\Delta e_{\mu\mu}$ values for various spin dimers are evaluated by performing EHTB calculations. For a variety of magnetic solids of transition metal ions it has been found that their magnetic properties are well described by the $<(\Delta e)^2>$ values obtained from EHTB calculations,[3-7] when both the d orbitals of the transition metal ions and the s/p orbitals of its surrounding ligands are represented by double-zeta Slater type orbitals (DZ-STO's). Our calculations are carried out using the atomic parameters summarized in the Table 1.

Table 1. Exponents ζ_i and valence shell ionization potentials H_{ii} of Slater-type orbitals χ_i used for EHTB calculations[a]

Atom	χ_i	H_{ii}	ζ_1	C_1[b]	ζ_2	C_2[b]
Fe	4s	−9.10	1.925	1.000		
Fe	4p	−5.32	1.390	1.000		
Fe	3d	−12.6	6.068	0.4038	2.618	0.7198
O	2s	−32.3	2.688	0.7076	1.675	0.3745
O	2p	−14.8	3.694	0.3322	1.659	0.7448
F	2s	−40.0	3.136	0.6737	1.945	0.4144
F	2p	−18.1	4.184	0.3546	1.851	0.7279
P	3s	−18.6	2.367	0.5846	1.499	0.5288
P	3p	−14.0	2.065	0.4908	1.227	0.5940
H	1s	−13.6	1.300	1.000		

[a]H_{ii}'s are the diagonal matrix elements $\langle\chi_i|H^{eff}|\chi_i\rangle$, where H^{eff} is the effective Hamiltonian. In our calculations of the off-diagonal matrix elements $H_{ij} = \langle\chi_i|H^{eff}|\chi_i\rangle$, the weighted formula was used. See: Ammeter, J.; Bürgi, H.-B.; Thibeault, J. C.; Hoffmann, R. *J. Am. Chem. Soc.* **1978**, *100*, 3686. [b]Contraction coefficients used in the double-ζ Slater-type orbital.

The radial part of a DZ-STO is expressed as r^{n-1} [$c_1 \exp(-\zeta_1 r) + c_2 \exp(-\zeta_2 r)$], where n is the principal quantum number, and the exponents ζ_1 and ζ_2 describe contracted and diffuse STO's, respectively (i.e., $\zeta_1 > \zeta_2$). The diffuse STO provides an orbital tail that enhances overlap between O atoms in the O···O contacts of the M–O···O–M SSE paths. The spin orbital interaction energy $\Delta e_{\mu\mu}$ values are affected most sensitively by the exponent ζ_2 of the diffuse O 2p orbital. The ζ_2 values taken from results of electronic structure calculations[13] for neutral atoms may not be diffuse enough to describe O^{2-} ions. To make the O 2p orbital more diffuse, the ζ_2 value should be reduced. To assess how the diffuseness of the O 2p orbital affects the relative strengths of the SSE interactions between adjacent FeO_3F_3 octahedra, we replace ζ_2 with $(1 \pm x)\zeta_2$ and calculate the $<(\Delta e)^2>$ values for three values of x, i.e., 0.00 and ±0.05.

In the SSE path J_2, two adjacent (FeO_3F_3) octahedral units are connected by corner-sharing through one (HPO_3) bridge. While in the SSE path J_1, two adjacent (FeO_3F_3) units are arranged in an edge-sharing manner through the (HPO_3) bridges (Figure 2). From the viewpoint of the magnetic orbital interactions, we can predict that the magnetic orbital interactions between the e_g-block orbitals of adjacent (FeO_3F_3) octahedra are much stronger than those caused by the t_{2g}-block orbitals, when the atoms consisting of Fe-O···O-Fe SSE path are aligned

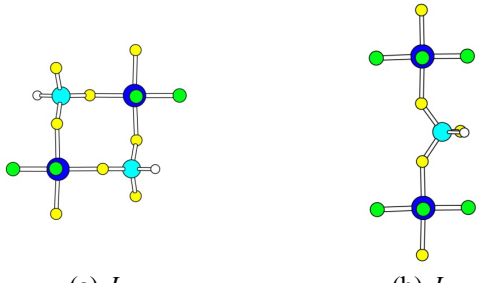

(a) J_1 (b) J_2

Figure 2. Spin dimers associated with the SSE paths (a) J_1 and (b) J_2 in $(C_2N_2H_{10})$[$Fe(HPO_3)F_3$].

Table 2. Relative values of $<(\Delta e)^2>$ obtained from EHTB calculations for $(C_2N_2H_{10})[Fe(HPO_3)F_3]$

Path	Fe···Fe (Å)	x = −0.05	x = 0.00	x = 0.05
J_1	4.891	0.07	0.06	0.11
J_2	6.438	1.00	1.00	1.00

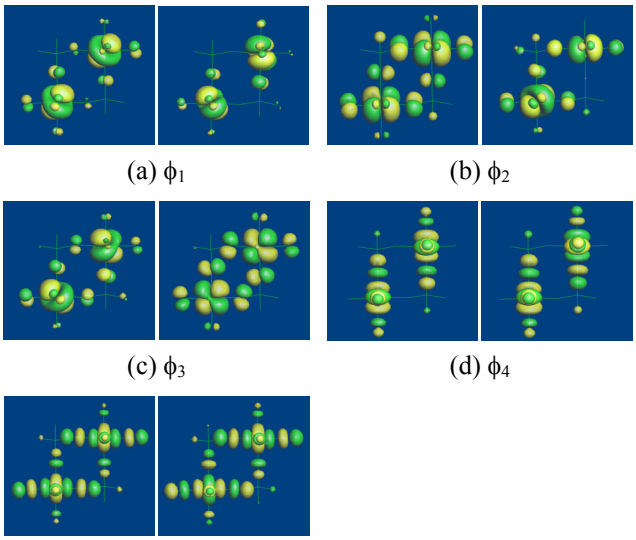

(a) ϕ_1 (b) ϕ_2 (c) ϕ_3 (d) ϕ_4 (e) ϕ_5

Figure 3. Pairs of magnetic orbitals defining the orbital interaction energies $(\Delta e_{\mu\mu})^2$ in the spin dimer representing the SSE path J_1.

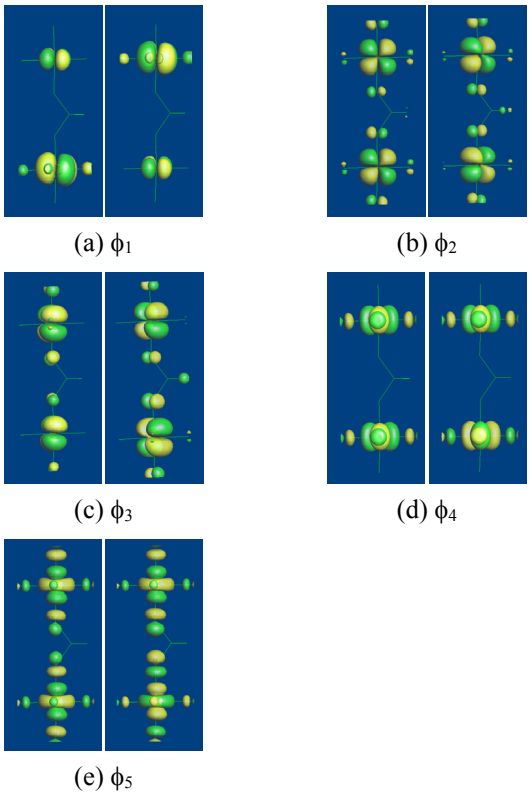

(a) ϕ_1 (b) ϕ_2 (c) ϕ_3 (d) ϕ_4 (e) ϕ_5

Figure 4. Pairs of magnetic orbitals defining the orbital interaction energies $(\Delta e_{\mu\mu})^2$ in the spin dimer representing the SSE path J_2.

linearly. In this arrangement, one of the magnetic orbital interactions between e_g-block levels is σ-type overlap which is much stronger than the π- or δ-type.[3,14] For the SSE path J_1, the spin exchange interaction is strongly affected by the orbital interactions between the t_{2g}-block levels. Comparing with the SSE path J_1, the spin exchange interaction of the SSE path J_2 is strongly affected by the orbital interaction between the e_g-block levels, especially for the σ-type overlap. Therefore, we expect the spin exchange interaction of the SSE J_2 is much stronger than that of the J_1. Table 2 shows the relative values of $<(\Delta e)^2>$ obtained from the spin dimer analysis based on EHTB calculations. The SSE path J_2 is strongly interacting spin dimer. This result is consistent with our prediction. The magnetic orbital interactions of the SSE paths J_1 and J_2 are represent in Figure 3 and Figure 4, respectively. As shown in Figure 4, the magnetic orbital interaction between the ϕ_5 orbitals is strong σ-type overlap. The tendency of spin exchange interactions in $(C_2N_2H_{10})[Fe(HPO_3)F_3]$ is not changed by the diffuseness of O 2p orbital.

Mapping Analysis

On the basis of first principles electronic structure theory, the spin exchange parameters of a magnetic solid are estimated either by calculating the electronic structures for the high- and low-spin states of various spin dimers of the solid or by calculating the electronic band structures for various ordered spin states of the solid.[3a,15-17] The energy differences between different electronic states are then mapped onto the corresponding energy differences given by the spin Hamiltonian employed. In either explaining trends in spin exchange interactions of magnetic solids or testing the validity of a set of spin exchange parameters chosen to form a spin Hamiltonian, however, it is sufficient to estimate the relative magnitudes of the spin exchange parameters.[3]

To determine the spin exchange parameters J_1 and J_2 on the basis of first principles DFT electronic band structure calculations, we first calculate the total energies of three ordered spin states (Figure 5) of $(C_2N_2H_{10})[Fe(HPO_3)F_3]$ and then relate the energy differences between these states to the corresponding energy differences expected from the spin Hamiltonian,

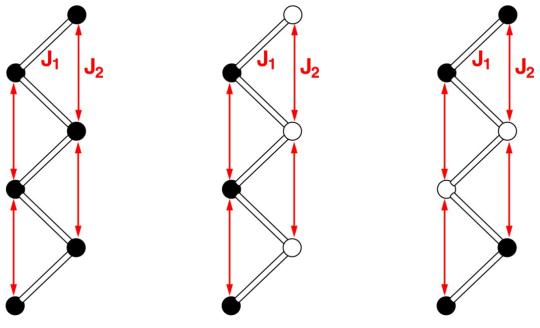

(a) FM (b) AF1 (c) AF2

Figure 5. Ordered spin arrangements (a) FM, (b) AF1, and (c) AF2. The black and large white circles refer to the up and down spin Fe sites, respectively.

Table 3. Relative energies (in meV) of three ordered spin states of $(C_2N_2H_{10})[Fe(HPO_3)F_3]$ obtained from GGA+U calculations

State	U = 5 eV	U = 6 eV	U = 7 eV
E_{FM}	72	59	47
E_{AF1}	60	50	40
E_{AF2}	0	0	0

$$\hat{H} = -\sum_{i<j} J_{ij}\hat{S}_i \cdot \hat{S}_j \tag{3}$$

where J_{ij} (= J_1 and J_2) is the spin exchange parameter for the spin exchange interaction between the spin sites *i* and *j*, while $\hat{S}_i$ and $\hat{S}_j$ are the spin angular momentum operators at the spin sites *i* and *j*, respectively. The total energies of these states were calculated by performing spin-polarized DFT electronic band structure calculations with the projected augmented-wave method encoded in the Vienna ab initio simulation package.[18] Our calculations employed the generalized gradient approximation (GGA) for the exchange and correlation correction,[19] the plane wave cut off energy of 450 eV, the on-site repulsion U on iron, and the sampling of the irreducible Brillouin zone with 96 k-points. To see how the value of U affects our results, we performed GGA plus onsite repulsion (GGA+U) calculations[20] with U = 5, 6, and 7 eV.

Our GGA+U calculations show that the AF2 state is the most stable state. The relative energies of the three ordered spin states with respect to that of the AF2 state are listed in Table 3. The trend in the relative energies does not change with the value of U employed. To extract the values of the spin exchange parameters J_1 and J_2 from the above electronic structure calculations, we express the total spin exchange interaction energies of the three ordered spin states in terms of the spin Hamiltonian given in Eq. (3). By applying the energy expressions obtained for spin dimers with *N* unpaired spins per spin site (in the present case, $N = 5$), the total spin exchange energies per formula units are written as[21]

$$\begin{aligned} E_{FM} &= (-8J_1 - 8J_2)N^2/4 \\ E_{AF1} &= (8J_1 - 8J_2)N^2/4 \\ E_{AF2} &= (8J_2)N^2/4 \end{aligned} \tag{4}$$

From the above equations, the spin exchange parameters J_1 and J_2 can be expressed in terms of state energy differences as follows:

$$\begin{aligned} J_1 &= \frac{1}{16}\left(\frac{4}{N^2}\right)(E_{AF1} - E_{FM}), \\ J_2 &= \frac{1}{16}\left[\left(\frac{4}{N^2}\right)(E_{AF2} - E_{AF1}) + 8J_1\right] \end{aligned} \tag{5}$$

The J_1 and J_2 values calculated from the above expressions are summarized in Table 4. For all values of U employed, the J_2 is much stronger than the J_1. This result confirms the prediction of the spin dimer analysis based on EHTB calculations.

Table 4. Values of spin exchange parameters (in K) and Curie-Weiss temperature (in K) of $(C_2N_2H_{10})[Fe(HPO_3)F_3]$ determined from GGA+U calculations

	U = 5 eV	U = 6 eV	U = 7 eV
J_1	−1.38	−1.08	−0.84
J_2	−7.62	−6.30	−5.04
θ_{cal}	−53	−43	−34

To determine how reasonable the calculated spin exchange parameters J_1 and J_2 are, we calculated the Curie-Weiss temperature θ in terms of these parameters. In the mean field theory,[22] which is valid in the paramagnetic limit, θ is related to the spin exchange parameters of $(C_2N_2H_{10})[Fe(HPO_3)F_3]$ as follows:

$$\theta = \frac{S(S+1)}{3k_B}\sum_i z_i J_i \tag{6}$$

where the summation runs over all nearest neighbors of a given spin site, z_i is the number of nearest neighbors connected by the spin exchange parameter J_i, and *S* is the spin quantum number of each spin site (i.e., $S = 5/2$ in the present case). Thus, by employing the spin site of each linear spin unit, θ can be approximated by

$$\theta \approx \frac{35}{12k_B}(2J_1 + 2J_2) \tag{7}$$

The θ values estimated by using the calculated spin exchange parameters (i.e., θ_{cal}) are summarized in Table 4. In magnitude, the θ_{cal} values are greater than the experimental value (i.e., −28.0 K) by a factor of approximately 2. The θ value estimated with J_1 and J_2 by Fernández-Armas *et al.*[2] is −14.6 K which is inconsistent with the experimental value. The overestimation of the θ_{cal} is not surprising because DFT electronic structure calculations generally overestimate the magnitude of spin exchange interactions by a factor approximately up to four.[3,17b,21a,23]

Concluding Remarks

Magnetic properties of $(C_2N_2H_{10})[Fe(HPO_3)F_3]$ were examined in terms of spin dimer analysis based on EHTB method as well as mapping analysis based on first principles DFT calculations. In the SSE path J_1 containing two (HPO_3) bridges, two adjacent $[FeO_3F_3]$ ions are arranged like an edge-sharing spin dimer, while for the SSE path J_2 the adjacent $[FeO_3F_3]$ ions are arranged linearly like a corner-sharing spin dimer. From the viewpoint of the magnetic orbital interaction we can predict the spin exchange interaction of the J_2 is much stronger than that of J_1 because the SSE path J_2 has the σ-type overlap. This prediction is verified with the result obtained from the spin dimer analysis based on EHTB calculations. From the mapping analysis, we also obtained much larger J_2 which is consistent with the results from the spin dimer analysis and magnetic orbital interactions. Both electronic structure calculations indicate that the spin exchange interaction of J_2 is stronger than the J_1. To confirm our results by performing the electronic structure cal-

culations, it is necessary to carry out inelastic neutron scattering measurements.

Acknowledgments. This research was supported by the Kyung Hee University Research Fund in 2007 (KHU-2007 0597).

References

1. Fernández, S.; Mesa, J. L.; Pizarro, J. L.; Lezama, L.; Arriortua, M. I.; Rojo, T. *Chem. Mater.* **2003**, *15*, 1204.
2. Fernández-Armas, S.; Mesa, J. L.; Pizarro, J. L.; Clemete-Juan, J. M.; Coronado, E.; Arriortua, M. I.; Rojo, T. *Inorg. Chem.* **2007**, *45*, 3240.
3. For reviews see: (a) Whangbo, M.-H.; Koo, H.-J.; Dai, D. *J. Solid State Chem.* **2003**, *176*, 417. (b) Whangbo, M.-H.; Dai, D.; Koo, H.-J. *Solid State Sci.* **2005**, *7*, 827.
4. Koo, H.-J.; Whangbo, M.-H. *Inorg. Chem.* **2005**, *44*, 4359.
5. Belik, A. A.; Koo, H.-J.; Whangbo, M.-H.; Tsujii, N.; Naumov, P.; Takayama-Muromachi, E. *Inorg. Chem.* **2007**, *46*, 8684.
6. Koo, H.-J.; Whangbo, M.-H. *Inorg. Chem.* **2008**, *47*, 4779.
7. Koo, H.-J.; Whangbo, M.-H. *Inorg. Chem.* **2010**, *49*, 9253.
8. (a) Johnston, D. C.; Johnson, J. W.; Goshorn, D. P.; Jacobson, A. J. *Phys. Rev. B* **1987**, *35*, 219. (b) Barnes, T.; Riera, J. *Phys. Rev. B* **1994**, *50*, 6817. (c) Eccleston, R. S.; Barnes, T.; Brody, J.; Johnson, J. W. *Phys. Rev. Lett.* **1994**, *73*, 2626. (d) Garret, A. W.; Nagler, S. E.; Tennant, D. A.; Sales, B. C.; Barnes, T. *Phys. Rev. Lett.* **1997**, *79*, 745.
9. (a) Koo, H.-J,; Whangbo, M.-H. *Inorg. Chem.* **2000**, *39*, 3699. (b) Koo, H.-J.; Whangbo, M.-H.; VerNooy, P. D.; Torardi, C. C.; Marshall, W. J. *Inorg. Chem.* **2002**, *41*, 4664. (c) Koo, H.-J.; Whangbo, M.-H. *Inorg. Chem.* **2006**, *45*, 4440 (d) Koo, H.-J.; Whangbo, M.-H. *Inorg. Chem.* **2008**, *47*, 128.
10. Hay, P. J.; Thibeault, J. C.; Hoffmann, R. *J. Am. Chem. Soc.* **1975**, *97*, 4884.
11. Hoffmann, R. *J. Chem. Phys.* **1963**, *39*, 1397.
12. Our calculations were carried out by employing the SAMOA (Structure and Molecular Orbital Analyzer) program package (Dai, D.; Ren, J.; Liang, W.; Whangbo, M.-H. http://chvamw.chem.ncsu.edu/, 2002).
13. Clementi, E.; Roetti, C. *At. Data Nucl. Data Tables* **1974**, *14*, 177.
14. Albright, T, A.; Burdett, J. K.; Whangbo, M.-H. *Orbital Interactions in Chemistry*; John Wiley & Sons: NY, 1985.
15. Noodleman, L. *J. Chem. Phys.* **1981**, *74*, 5737.
16. Illas, F.; Moreira, I. de P. R.; de Graaf, C.; Barone, V. *Theor. Chem. Acc.* **2000**, *104*, 265.
17. (a) Chartier, A.; D'Arco, P.; Dovesi, R.; Saunders, V. R. *Phys. Rev. B* **1999**, *60*, 14042. (b) Dai, D.; Whangbo, M.-H.; Koo, H.-J.; Rocquefelte, X.; Jobic, S.; Villesuzanne, A. *Inorg. Chem.* **2005**, *44*, 2407.
18. (a) Kresse, G.; Hafner, J. *Phys. Rev. B* **1993**, *47*, 558. (b) Kresse, G.; Furthmüller, J. *Comput. Mater. Sci.* **1996**, *6*, 15. (c) Kresse, G.; Furthmüller, J. *Phys. Rev. B* **1996**, *54*, 11169.
19. Perdew, J. P.; Burke, J.; Ernzerhof, M. *Phys. Rev. Lett.* **1996**, *77*, 3865.
20. Dudarev, S. L.; Botton, G. A.; Savrasov, S. Y.; Humphreys, C. J.; Sutton, A. P. *Phys. Rev. B* **1998**, *57*, 1505.
21. (a) Dai. D.; Whangbo, M.-H. *J. Chem. Phys.* **2001**, *114*, 2887. (b) Dai. D.; Whangbo, M.-H. *J. Chem. Phys.* **2003**, *118*, 29.
22. Smart, J. S. *Effective Field Theory of Magnetism*; Saunders: Philadelphia, 1966.
23. Grau-Crespo, R.; de Leeuw, N. H.; Catlow, C. R. *J. Mater. Chem.* **2003**, *13*, 2848.